



Contents lists available at ScienceDirect

# Journal of Food Engineering

journal homepage: [www.elsevier.com/locate/jfoodeng](http://www.elsevier.com/locate/jfoodeng)



## A mathematical model for packaging with microperforated films of fresh-cut fruits and vegetables

Jaime González-Buesa, Ana Ferrer-Mairal, Rosa Oria, María L. Salvador \*

Laboratory of Vegetal Food, University of Zaragoza, Miguel Servet 177, 50013 Zaragoza, Spain

### ARTICLE INFO

*Article history:*  
Received 3 February 2009  
Received in revised form 22 April 2009  
Accepted 25 April 2009  
Available online xxxx

*Keywords:*  
MAP  
Gas exchange  
Respiration rate  
Peach  
Cauliflower  
Truffle

### ABSTRACT

For the design of modified atmosphere packaging with microperforated films it is necessary to know the respiratory kinetics of the product and the gas interchange through the packaging. The aim of this work was to describe an empirical equation that relates the microperforation area with the transmission rate in order to present a mathematical model, valid for packages of constant volume. The model should take into account the dependency of the respiration rate with the gas composition and the existence of a hydrodynamic flow through the microperforations. The evolution of the gas composition inside the package predicted by the model has been compared with the results of experiments conducted at 4 °C with minimally processed peach ('Andross' and 'Calante' cultivars), fresh-cut cauliflower and whole black truffle, by using seven packages of different number (0–14) and size (from 90 × 50 μm to 300 × 100 μm) of microperforations. The respiratory kinetics of these products was previously determined in a closed system. It has been established that the rate of O<sub>2</sub> consumption is a potential function of the O<sub>2</sub> concentration, while the production of CO<sub>2</sub> is linear, except in the case of the truffle which showed a linear dependency for O<sub>2</sub> and CO<sub>2</sub>. The experimental data and those predicted by the model showed a satisfactory agreement for the O<sub>2</sub>, while the CO<sub>2</sub> is underestimated for products with RQ < 1 but in agreement when RQ > 1. The reason for this behaviour could be the CO<sub>2</sub> concentration gradient within the package owing to the air flow that moves to compensate pressure differences.

© 2009 Published by Elsevier Ltd.

### 1. Introduction

Modified atmosphere packaging (MAP) of minimally processed fruits and vegetables combined with cold storage are considered as the best way to maintain sensory and microbiological quality of fresh-cut produce (Kader et al., 1989; Philips, 1996). Low O<sub>2</sub> and elevated CO<sub>2</sub> atmospheres reduce the product respiration rate (Watada et al., 1996), while the CO<sub>2</sub> accumulation favours the inhibition of microbial growth responsible for product deterioration (Bennik et al., 1998).

Modified atmosphere design (MAP) for fruit and vegetables is a complex task requiring an understanding of the dynamic interactions established between the product, the atmosphere generated within the package and the package itself (Yam and Lee, 1995). A large number of variables should be integrated: the respiration rate of the product as a function of the temperature, the optimum gas composition and tolerance limits, gas transport through the package depending on the temperature, gas exchange area, free volume, weight of the product, etc. Mathematical models are useful tools for defining the characteristics that a package should have and

for predicting the evolution of the gas composition during conservation of the product.

Many of the early models developed for modified atmosphere packaging concentrated on the analysis of equilibrium atmospheres (Mannapperuma et al., 1989; Emond et al., 1991; Cameron et al., 1994; Talasila et al., 1994). However, for minimally processed products in particular, the time required to reach this equilibrium can represent a significant percentage of their short useful life (7–9 days). Furthermore, in some circumstances the CO<sub>2</sub> can reach a maximum concentration different from that of equilibrium, especially if films with a high permeability quotient,  $\beta = Q_{CO_2}/Q_{O_2}$ , are used (Fishman et al., 1995; Salvador et al., 2002). The products are therefore subjected to CO<sub>2</sub> concentrations higher than their tolerance limit, despite the fact that the concentrations in the equilibrium might or might not be adequate.

As the use of perforated films became more widespread as an alternative to overcome the limitations of conventional polymeric films, research works began to be published about the modelling of gas exchange in this type of packaging. However, the majority of these studies (Emond et al., 1991; Fishman et al., 1996; Fonseca et al., 1996; Lange et al., 2000; Paul and Clarke, 2002) referred to quite large perforations (from 0.2 up to 17 mm in diameter). The high respiration rate of minimally processed products requires much greater permeability than that provided by unperforated

\* Corresponding author. Tel.: +34 976 762739; fax: +34 976 761612.  
E-mail address: [mlsalva@unizar.es](mailto:mlsalva@unizar.es) (M.L. Salvador).

## Nomenclature

$a_1, a_2$	constants	$R$	gas constant ( $\text{Pa m}^3 \text{ mol}^{-1} \text{ K}^{-1}$ )
$A$	film area ( $\text{m}^2$ )	$R_i$	respiration rate expressed as consumption or production of a gas $i$ ( $\text{m}^3 \text{ kg}^{-1} \text{ s}^{-1}$ )
$A_h$	microperforation area ( $\text{m}^2$ )	$R_{O_2}$	respiration rate expressed as consumption of $O_2$ ( $\text{m}^3 \text{ kg}^{-1} \text{ s}^{-1}$ )
$CO_2$	carbon dioxide concentration (%)	$R_{CO_2}$	respiration rate expressed as production of $CO_2$ ( $\text{m}^3 \text{ kg}^{-1} \text{ s}^{-1}$ )
$d$	diameter of the microperforation ( $\mu\text{m}$ )	$t$	time (s)
$J_{fi}$	transmission of gas $i$ across the film ( $\text{mol s}^{-1}$ )	$T$	temperature (K)
$J_{hi}$	flow of gas $i$ through the holes ( $\text{mol s}^{-1}$ )	$TR_i$	gas $i$ transmission rate ( $\text{m}^3 \text{ s}^{-1}$ )
$J_i$	total permeation flow of gas $i$ through the film ( $\text{mol s}^{-1}$ )	$V$	free package volume ( $\text{m}^3$ )
$J_{p,i}$	hydrodynamic flow of gas $i$ ( $\text{mol s}^{-1}$ )	$W$	product mass (kg)
$L$	thickness of the film (m)	$\lambda$	molecular mean free path (m)
$n_i$	moles of gas $i$	$\mu$	gas viscosity ( $\text{Pa s}^{-1}$ )
$O_2$	oxygen concentration (%)		adjustable parameters: $m, n, q, s$
$P$	pressure (Pa)		
$p_i$	partial pressure of gas $i$ inside the package (Pa)		
$p_{i,out}$	partial pressure of gas $i$ outside the package (Pa)		
$Q_i$	gas $i$ permeability coefficient of the polymeric film ( $\text{m}^2 \text{ s}^{-1} \text{ Pa}^{-1}$ )		

films. In addition, perforated films have a permeability quotient close to 1 (Brody, 2005) and this allows the required concentrations of  $CO_2$  to be reached without anaerobiosis, taking into account that the respiration coefficient of the product can fluctuate between 0.7 and 1.3 (Kader, 1987). These factors justify the interest in using perforated films. However, the size of the perforations normally used in MAP is between 50 and 200  $\mu\text{m}$  in diameter, appreciably smaller than the sizes referred to above. The extrapolation of predictions of gas transmission obtained with the sizes referred above to microperforations could lead to errors which directly affect the composition of the package atmosphere. It is therefore important to quantify the influence of the microperforation size, total exchange area, equivalent radius and film thickness on the gas transmission rate. In a previous work (González et al., 2008), an empirical equation that relates the area of a microperforation with the transmission rate of oxygen and carbon dioxide was derived from experimental data. The results were compared with other experimental data (Ghosh and Ananteswaran, 2001) and with those predicted by five other models (Heiss, 1954; Becker, 1979; Emond et al., 1991; Fishman et al., 1996; Fonseca et al., 1996). The  $O_2$  and  $CO_2$  transmission rates predicted by the empirical equation were very close to those obtained with the modified Fick's equation in which the total diffusive pass length of a perforation is considered as the sum of the perforation length and a correction factor, which is approximately 0.5 times the diameter of the perforation. Unlike the other proposed equations, this equation can be used for a wide range of conditions (diameters between 40  $\mu\text{m}$  and 10 mm, and thicknesses between 30  $\mu\text{m}$  and 1.5 mm). The aim of this work is to verify experimentally the gas exchange predictions through microperforated films with packages containing minimally processed products. To achieve this objective, first the respiration kinetics of the products were determined. These measurements are considered necessary for the following reasons: (i) fresh-cut products have a physiology that differs from intact produce (Martínez et al., 2005), (ii) the respiration rates given in the literature do not always take into account their dependence on the gas composition while MAP design for fresh-cut produce requires a suitable model for the prediction of the respiration rate as a function of the gas composition (Iqbal et al., 2009; Fonseca et al., 2002) and (iii) the respiration activity varies with the cultivars. A mathematical model is subsequently proposed that takes into account the physiological activity of the products, the diffusive flow through the microperforations, the film permeability, as well as the

hydrodynamic flow to compensate for the differences in pressure. Finally, the experimentally measured evolution of the gas compositions in the interior of the packages is compared with those predicted by the model.

## 2. Material and methods

### 2.1. Preparation of produce

The two cultivars of peach, 'Andross' and 'Calante', were harvested at commercial maturity stage (soluble solids:  $13.6 \pm 1.7^\circ$  Brix for 'Andross' and  $11.4 \pm 0.9^\circ$  Brix for 'Calante'; acidity:  $5.1 \pm 0.1$  g/L in 'Andross' and  $6.1 \pm 1.0$  g/L in 'Calante'; firmness in penetration test with cylindrical punch of 6 mm diameter:  $5.7 \pm 1.0$  kg  $\text{cm}^{-2}$  for 'Andross' and  $3.6 \pm 0.4$  kg  $\text{cm}^{-2}$  for 'Calante'). Upon arrival at the laboratory they were refrigerated to a temperature of  $0-1^\circ\text{C}$ , after which they were disinfected (100 ppm active chlorine, 5 min) to reduce the surface microbial charge and left to drain for 10 min. The peaches were peeled with a semi-automatic peeler (Orange Peel model, Pelamatic). The stones were removed with a manual corer, while a special Granton fruit knife was used to cut them into 10–12 slices. They were immersed during 30 min in a cold bath ( $2^\circ\text{C}$ ) containing 2% ascorbic acid, 1% citric acid and 1% calcium chloride. The segments were then immediately drained cold on a sieve for 15 min.

The cauliflower, *Brassica oleracea* var. *Botrytis* L. of the 'Meridien' cultivar, was supplied by a local distributor (Cooperativa San Lamberto, Zaragoza, Spain). The approximate mass of the cauliflowers was 900 g, with a diameter of 15 cm. The leaves were removed and any cauliflowers with blemishes or in bad condition were rejected. They were cut into 15–20 g pieces with a knife (Granton, UK). Afterwards they were washed (at  $2^\circ\text{C}$ , with 100 ppm of active chlorine, 5 min) and drained for 10 min.

The black truffles (*Tuber melanosporum*) used in this study were obtained from artificial truffle grounds in Teruel (Spain). The truffles, dug with the help of trained truffle dogs, were all at a similar stage of maturity and surrounded by a layer of soil in insulated boxes with ice bags and transported immediately to our laboratory. Upon arrival, the soil was removed by brushing the truffles with a wet soft brush. They were then rinsed with tap water and dried in a fluid laminar cabinet. Qualitative selection of the carpophores was made by discarding truffles with softened texture, dip-

ters and coleoptera larva or those extremely damaged during the harvest.

All the products were cooled to a temperature of 4 °C prior to having the respiration rate measured.

### 2.2. Closed system respiration experiments

The respiration rate was determined in a closed system at 4 °C. A quantity of product (0.5 kg of peach, 0.345 kg of cauliflower or 0.050 kg of truffle) was placed in hermetic containers (1230 mL capacity for peach and cauliflower and 250 mL for truffles), and both the consumption of O<sub>2</sub> and the production of CO<sub>2</sub> were measured. The composition of the gas inside the containers was determined with a Hewlett Packard 4890 (Geneva, Switzerland) gas chromatograph equipped with a thermal conductivity detector and a CP-Carboplot Chrompack (Bergen op Zoom, Norwegian) capillary column of 25 m in length with a film thickness of 25 μm, and an internal and external diameter of 0.53 mm and 0.75 mm, respectively. Helium was used as a carrier gas (12.6 mL min<sup>-1</sup>). The monitoring of the evolution of the gaseous composition in the interior of the containers was done by triplicate until the O<sub>2</sub> levels reached 1%. The results shown (Figs. 1 and 2) are average values of the three measurements taken.

### 2.3. Packages

The Amcor P-Plus (Amcor Flexibles, Ledbury, UK) films used have a polymeric matrix, made up of one layer of low density polyethylene and another of polyester, and microperforations of different sizes. Using equipment based on the ASTM D3985-05 norm, the permeability coefficients of the matrix, Q<sub>i</sub>, were experimentally obtained at 4 °C. The thickness of the film, 40 μm, was determined as the average of five measurements with a Mitutoyo (Kawasaki, Japan) gauge. The size of the microperforations was measured with a Zeiss (Thornwood, NY, USA) microscope provided with a calibrated ocular micrometer. The sizes of the microperforations were between 90 × 50 and 200 × 100 μm.

The products were placed in polypropylene trays wrapped in polyethylene, which can be considered as a barrier to gas transmission effects (during the market life of the product). The upper part of the package (96 cm<sup>2</sup>) was heat sealed with the microperforated film described above. The volume of the package and the weight of the product in each case was: 500 mL and 185 g for 'Andross' peach, 700 mL and 250 g for 'Calante' peach, 600 mL and 200 g

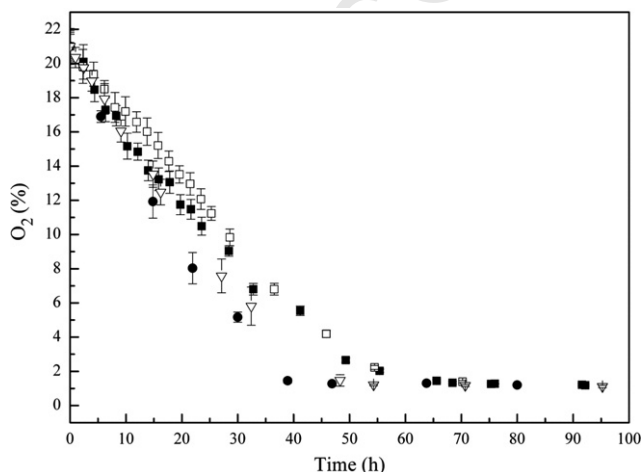


Fig. 1. Time course of O<sub>2</sub> depletion in the closed container atmosphere containing fresh-cut peach (■ 'Calante', □ 'Andross'), cauliflower (●) or truffle (▽).

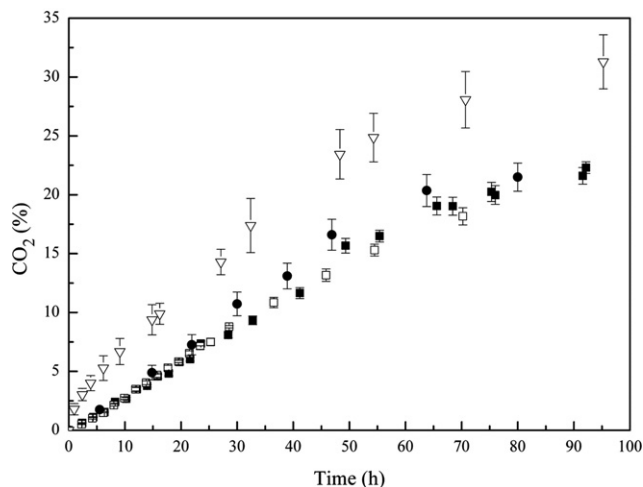


Fig. 2. Time course of CO<sub>2</sub> accumulation in the closed container atmosphere containing fresh-cut peach (■ 'Calante', □ 'Andross'), cauliflower (●) or truffle (▽).

for cauliflower, and 250 mL and 50 g for black truffle. The initial gas composition was similar to that of the atmosphere. Samples were kept in a cold room (4 °C, 80% RH).

### 2.4. Mathematical model

The model was developed for packages whose volume remains constant. The physiological activity of the product together with the gaseous exchange through the film are the two processes that contribute to the change in quantity of moles of a gas *i* (*n<sub>i</sub>*) in the interior of a package containing fruit or vegetables:

$$\frac{dn_i}{dt} = R_i W \frac{P}{RT} + J_i \quad (1)$$

where *R<sub>i</sub>* is the respiration rate, *W* is the product weight, *P* the pressure, *T* the temperature, *R* the gas constant, and *J<sub>i</sub>* is the total permeation flow through the film. In the case of microperforated films the total flow is:

$$J_i = J_{fi} + J_{hi} \quad (2)$$

where *J<sub>hi</sub>* is the flow of a gas *i* through the holes and *J<sub>fi</sub>* is the transmission of a gas *i* across the film, and can be expressed as (Geankoplis, 1993):

$$J_{fi} = - \frac{Q_i A (p_i - p_{i,out})}{L} \frac{P}{RT} \quad (3)$$

where *p<sub>i</sub>* and *p<sub>i,out</sub>* are the partial pressures of gas *i* inside and outside the package, *L* is the thickness of the polymeric film, *A* is the film area, and *Q<sub>i</sub>* is the gas *i* permeability coefficient of the polymeric film.

The flow of the gas *i* through the perforation, *J<sub>hi</sub>*, has been considered to be produced by two mechanisms (Hernandez, 1997; Del-Valle et al., 2003): ordinary diffusion (*d/λ* ≥ 100) and hydrodynamic flow, *J<sub>p,i</sub>*, resulting from the changes in pressure caused by a respiration coefficient different to one. The diffusion flow is itself the result of two magnitudes: the molar flow resulting from the overall movement of the fluid and the flow resulting from the diffusion superimposed on the overall flow (Bird et al., 2007):

$$J_{h,i} = \frac{p_i}{P} \sum_{i=1}^n J_{h,i} - TR_i \frac{(p_i - p_{i,out})}{RT} + J_{p,i} \quad (4)$$

where *TR<sub>i</sub>* is the transmission rate of gas *i* and which according to the results obtained in a previous study (González et al., 2008) can be expressed as:

$$TR_i = a_{1,i} \cdot A_h^{a_{2,i}} \quad (5)$$

$A_h$  being the microperforation area, and  $a_1, a_2$  constants for each gas  $i$ . The values of the constants are determined from the experimental data obtained at 23 °C ( $a_{1,O_2} = 0.880 \pm 0.111$ ,  $a_{2,O_2} = 0.577 \pm 0.0132$  with  $r^2 = 0.988$  for  $O_2$ ;  $a_{1,CO_2} = 0.830 \pm 0.111$ ,  $a_{2,CO_2} = 0.569 \pm 0.0140$  with  $r^2 = 0.986$  for  $CO_2$  and  $a_{1,N_2} = 1.169 \pm 0.253$ ,  $a_{2,N_2} = 0.558 \pm 0.0195$  with  $r^2 = 0.984$  for  $N_2$ ). For its use at another temperature, in respect of ordinary diffusion, the transmission rate is considered proportional to  $T^{3/2}$ . The validity of Eq. (5) (experimentally determined for  $L < 60 \times 10^{-6}$  m and  $A_h < 3.8 \times 10^{-8}$  m<sup>2</sup>) has been checked for  $L < 1.5 \times 10^{-3}$  m and  $A_h < 7.8 \times 10^{-5}$  m<sup>2</sup>, comparing it with the empirical equations in this interval proposed by other authors (González et al., 2008).

The hydrodynamic flow of gas  $i$  can be described by Poiseuille's law in laminar flow conditions:

$$\text{If } P_{out} > P_{p,i} = \frac{\pi d^4 (P_{out} - P) p_{i,out}}{128 \mu L} \frac{1}{RT} \quad (6)$$

$$\text{If } P_{out} < P_{p,i} = \frac{\pi d^4 (P_{out} - P) p_i}{128 \mu L} \frac{1}{RT} \quad (7)$$

where  $d$  is the microperforation diameter,  $P_{out} - P$  is the pressure differential and  $\mu$  is the gas viscosity.

### 3. Results and discussion

The respiratory kinetics have been determined from the results obtained in the closed system experiments. Figs. 1 and 2 show the evolution over time of the  $O_2$  and  $CO_2$  concentrations for the four products. Given that in each case the free volume/weight ratio of the product ( $V/W$ ) is different, from these data it is not possible to arrive directly at comparative conclusions regarding the respiration rate of the various products, though the high  $CO_2$  production in the case of the truffle can be remarked on.

The respiration rates for each product were calculated using these equations:

$$R_{O_2} = -\frac{1}{W} \frac{V}{100} \frac{dO_2}{dt} \quad (8)$$

$$R_{CO_2} = \frac{1}{W} \frac{V}{100} \frac{dCO_2}{dt} \quad (9)$$

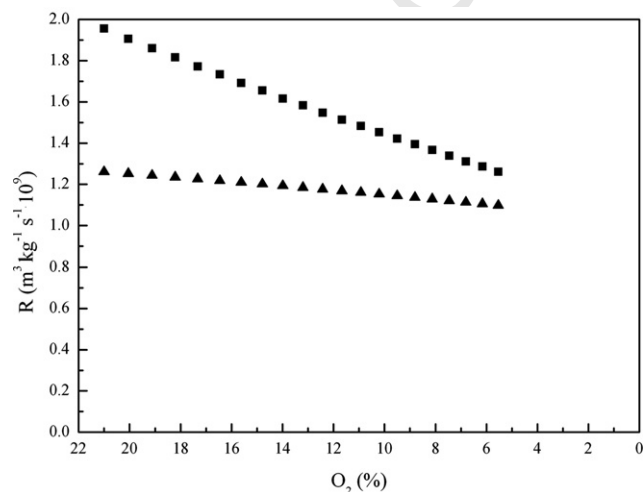


Fig. 3. Respiration rate of 'Andross' peach at 4 °C expressed as  $O_2$  consumption (■) and  $CO_2$  production (▲), versus  $O_2$  concentration.

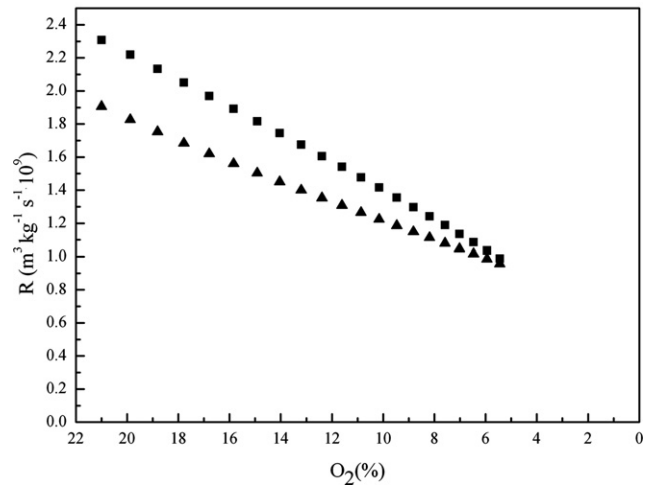


Fig. 4. Respiration rate of 'Calante' peach at 4 °C expressed as  $O_2$  consumption (■) and  $CO_2$  production (▲), versus  $O_2$  concentration.

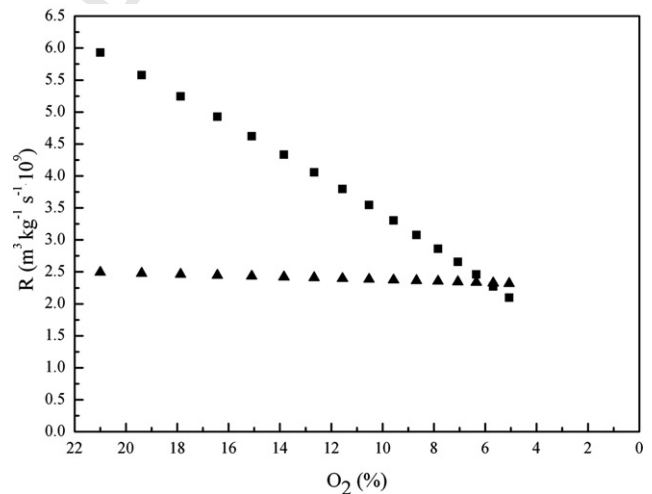


Fig. 5. Respiration rate of cauliflower at 4 °C expressed as  $O_2$  consumption (■) and  $CO_2$  production (▲), versus  $O_2$  concentration.

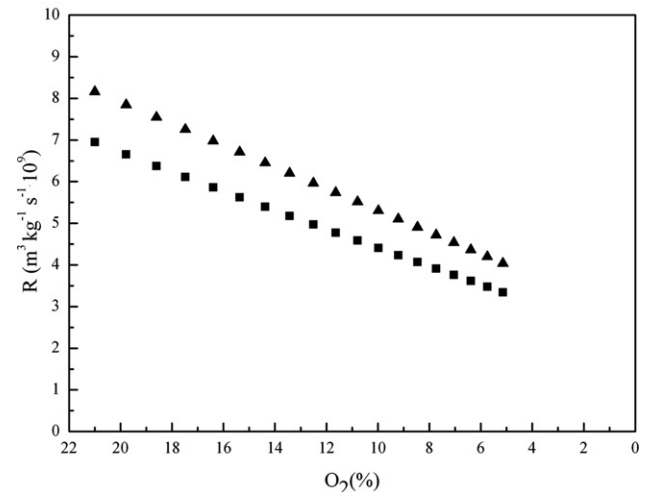


Fig. 6. Respiration rate of black truffle at 4 °C expressed as  $O_2$  consumption (■) and  $CO_2$  production (▲), versus  $O_2$  concentration.

**Table 1**  
Parameters  $m$ ,  $n$ ,  $q$  and  $s$  (Eqs. (12) and (13)) for the different products.

Product	$m$	$n$	$r^2$	$q$	$s$	$r^2$
Andross	2.559	0.318	0.972	0.0383	3.753	0.998
Calante	1.192	0.632	0.998	0.216	2.230	0.999
Cauliflower	2.287	0.732	0.999	0.0399	8.158	0.997
Truffle	0.814	7.778	0.999	0.936	9.751	0.999

The respiration rates thus obtained are shown in Figs. 3–6. In all cases a decrease in the respiration rate was observed as the oxygen concentration diminishes. In air, the respiration rate of the minimally processed ‘Calante’ peach is greater than that of the ‘Andross’, but the dependence of the latter on the oxygen concentration is less marked. The cauliflower initially shows a low respiratory quotient,  $R_{CO_2}/R_{O_2} = 0.42$ , but owing to the reduced dependence of the  $CO_2$  production rate on the oxygen concentration, this ratio increases up to 1.1. The truffle is the product with the highest respiration rate, even though it is not a fresh-cut product, managing to consume oxygen 3.5 times more quickly than the ‘Andross’ peach and to produce  $CO_2$  at a rate 6.5 times greater, showing respiration coefficients always greater than 1 (1.18–1.20). The respiration of vegetables is an enzymatic process, but it was decided to use equations which provide a good fit with the experimental values without any mechanistic background. Using a Michaelis–Mentel type equation resulted in very large values for the  $V_m$  parameter (maximum respiration rate) given that at high oxygen concentrations the inverse of the respiration rate has values close to zero. The respiration rate expressed as consumption of  $O_2$  is considered to vary potentially with the  $O_2$  concentration for the two peach cultivars and the cauliflower:

$$R_{O_2} = m \cdot O_2^n \quad (10)$$

while for the truffle the dependence is linear. In all cases, the rate of  $CO_2$  production is also linear:

$$R_{CO_2} = q \cdot O_2 + s \quad (11)$$

The values of the parameters  $m$ ,  $n$ ,  $q$  and  $s$  are shown in Table 1 for the different products.

Taking the above equations into account, and specifying for each of the gases involved, the differential equations that describe the variation over time of the number of moles of  $O_2$ ,  $CO_2$  and  $N_2$  inside a microperforated package containing a product with a specific respiratory activity are:

$$\frac{dn_{O_2}}{dt} = \frac{TR_{O_2}}{RT} (p_{O_2, out} - p_{O_2}) + \frac{p_{O_2}}{P} (J_{h, O_2} + J_{h, CO_2} + J_{h, N_2}) + \frac{Q_{O_2} A \cdot P}{RT L} (p_{O_2, out} - p_{O_2}) - R_{O_2} \frac{P}{RT} W + J_{p, O_2} \quad (12)$$

$$\frac{dn_{CO_2}}{dt} = \frac{TR_{CO_2}}{RT} (p_{CO_2, out} - p_{CO_2}) + \frac{p_{CO_2}}{P} (J_{h, O_2} + J_{h, CO_2} + J_{h, N_2}) + \frac{Q_{CO_2} A \cdot P}{RT L} (p_{CO_2, out} - p_{CO_2}) + R_{CO_2} \frac{P}{RT} W + J_{p, CO_2} \quad (13)$$

$$\frac{dn_{N_2}}{dt} = \frac{TR_{N_2}}{RT} (p_{N_2, out} - p_{N_2}) + \frac{p_{N_2}}{P} (J_{h, O_2} + J_{h, CO_2} + J_{h, N_2}) + \frac{Q_{N_2} A \cdot P}{RT L} (p_{N_2, out} - p_{N_2}) + J_{p, N_2} \quad (14)$$

Given that the volume of the package has been considered to remain constant, the pressure in its interior,  $P$ , can be calculated with the expression:

$$P = \frac{(n_{O_2} + n_{CO_2} + n_{N_2})RT}{V} \quad (15)$$

**Table 2**  
Values of the parameters used in Eqs. (12)–(14).

$Q_{O_2}$ ( $m^2 s^{-1} Pa^{-1}$ )	$4.04 \times 10^{-19}$		
$Q_{CO_2}$ ( $m^2 s^{-1} Pa^{-1}$ )	$1.32 \times 10^{-18}$		
$Q_{N_2}$ ( $m^2 s^{-1} Pa^{-1}$ )	$4.22 \times 10^{-19}$		
$P_{out}$ (Pa)	98,792		
Hole	$TR$ ( $m^3 s^{-1} \times 10^{11}$ )		
	$O_2$	$CO_2$	$N_2$
One $90 \times 50 \mu m$	102	90	117
Two $90 \times 50 \mu m$	204	180	234
Two $125 \times 75 \mu m$	234	205	259
One $200 \times 130 \mu m$	282	246	311
One $210 \times 135 \mu m$	298	259	327
Two $200 \times 120 \mu m$	404	349	438
Three $200 \times 100 \mu m$	458	397	496
Fourteen $150 \times 80 \mu m$	830	712	882

A fourth-order Runge–Kutta method has been used for the numerical solution of these differential equations. Table 2 shows the values of the parameters used in the calculations. The solution allows the prediction of the evolution of the gas composition inside the microperforated package.

To verify the suitability of the model, and to check whether it is capable of a good prediction of the behaviour of the package atmosphere, the experimental results have been compared with those obtained from the Eqs. (12)–(15). The model gives a correct description of the evolution of the oxygen concentration in all the products and films used (Figs. 7–10). For the two varieties of peach, extreme permeability conditions have been used ranging from a small package microperforation ( $90 \times 50 \mu m$ ) or even packages without microperforations, to three microperforations of relatively large sizes ( $200 \times 100 \mu m$ ). This meant that it was possible to obtain very different equilibrium gas compositions for the different types of packages tested and simulated, checking the validity of the proposed model for a large number of situations. Anoxia conditions were reached quickly with films without microperforations, while for packages with high effective permeability the concentration of oxygen in equilibrium is higher than would be recommended for this type of product (Gorny et al., 1999). In the case of the truffle (Fig. 10), a wide disparity was recorded in the experimental results due to the peculiarities of a very heterogeneous product. In any case, the theoretical predictions were within the interval defined by standard deviation.

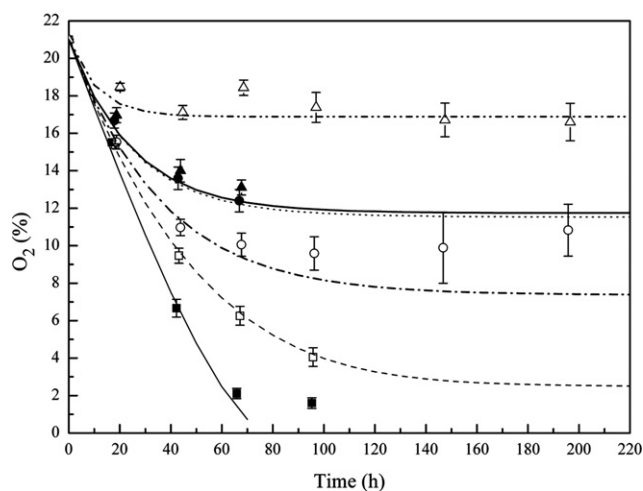


**Fig. 7.** Experimental and predicted evolution of  $O_2$  composition for different ‘Andross’ peach packages: without microperforation (■, continuous line), one  $90 \times 50 \mu m$  hole (□, dash line), two  $90 \times 50 \mu m$  holes (○, dash dot line), one  $210 \times 135 \mu m$  hole (●, dot line), two  $125 \times 75 \mu m$  holes (▲, continuous thick line), three  $200 \times 100 \mu m$  holes (△, dash dot dot line).

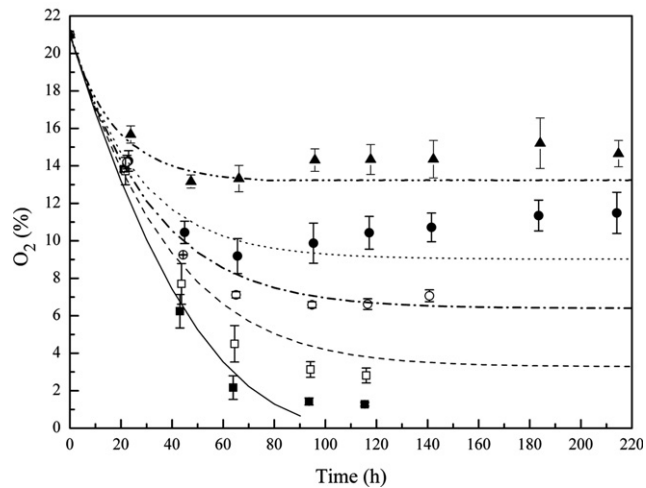


**Fig. 8.** Experimental and predicted evolution of O<sub>2</sub> composition for different 'Calante' peach packages: without microperforation (■, continuous line), one 90 × 50 μm hole (□, dash line), two 90 × 50 μm holes (○, dash dot line), one 200 × 130 μm hole (●, dot line), two 200 × 120 μm holes (▲, dash dot dot line).

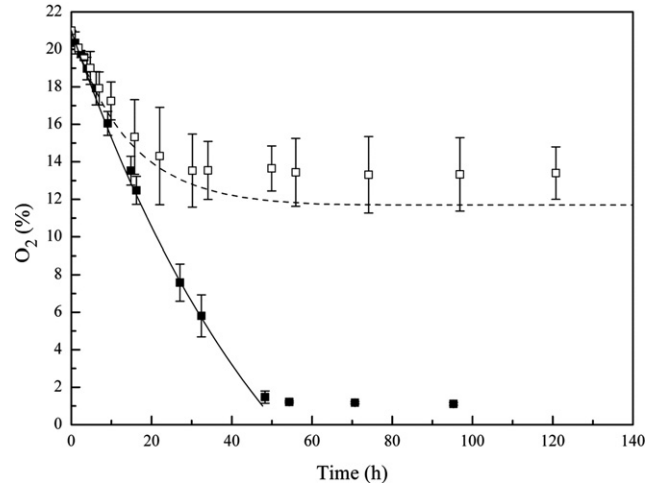


**Fig. 10.** Experimental and predicted evolution of O<sub>2</sub> composition for black truffle packages: without microperforation (■, continuous line), two 90 × 50 μm holes (□, dash line).

Regarding CO<sub>2</sub>, the model is not able to describe its evolution when there are microperforations in the packages of peach and cauliflower (Figs. 9, 11 and 12). For example, for the 'Andross' variety the estimated CO<sub>2</sub> concentration for packages with perforations of 90 × 50 μm correspond to the experimental results when there are two perforations of this same size. For the 'Calante' variety, the predictions for packages with a perforation of 200 × 130 μm agree with the experimental results for two perforations of 200 × 120 μm. These discrepancies are also observed for the cauliflower, where again the calculated results are lower than the experimental values. The respiratory kinetics do not appear to be the reason given that the model provides acceptable predictions of data obtained for packages without microperforations. The coefficient between the transmission rates of the CO<sub>2</sub> and the O<sub>2</sub> is 0.89 ± 0.05, coming within values obtained by other authors (Emond et al., 1991; Silva et al., 1999). However, it was observed experimentally that when a microperforation of 90 × 50 μm is incorporated, the CO<sub>2</sub> concentration changes very little compared to that obtained when there are no microperforations, while the O<sub>2</sub> concentration is more substantially modified. The reduction of

the CO<sub>2</sub> transport through the microperforations compared to the estimated value, which brings about a greater accumulation of this component, could be due to the entry of a continuous air flow inside the package as a consequence of a difference in pressure generated by the respiratory activity of the product. The respiratory coefficient of the peach and the cauliflower is lower than 1, which causes a depression inside the package that is immediately compensated for by the entry of air from the outside through hydrodynamic flow. This entry of air can generate in the area around the perforation a CO<sub>2</sub> concentration appreciably different to that existing inside the package. The real diffusive flow of CO<sub>2</sub> through the perforation would be lower than the estimated value if on the internal side of the perforation the concentration was the same as that existing near the product. The hydrodynamic flow would also have an effect on the oxygen, but in this case the 'sweeping' effect of the air to the entrance would be lower given that the diffusion goes in the same direction as the hydrodynamic flow. If the difference in pressure between the exterior and the interior of the package was null, or rather if the hydrodynamic flow went in the

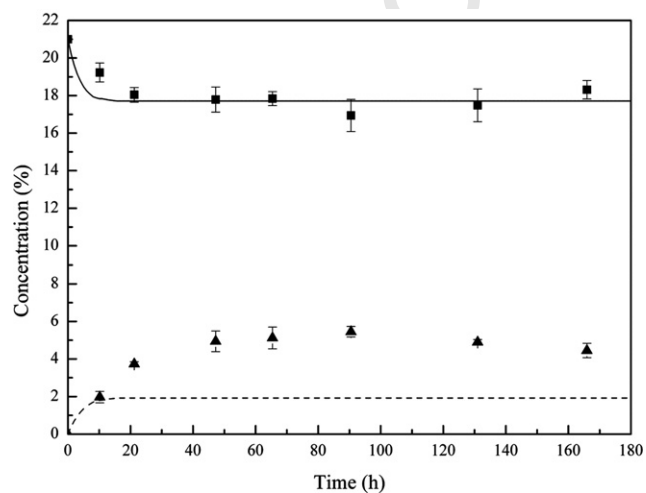


**Fig. 9.** Experimental and predicted evolution of gas composition for cauliflower inside packages with fourteen 150 × 80 μm holes: O<sub>2</sub> (■, continuous line) and CO<sub>2</sub> (▲, dash line).

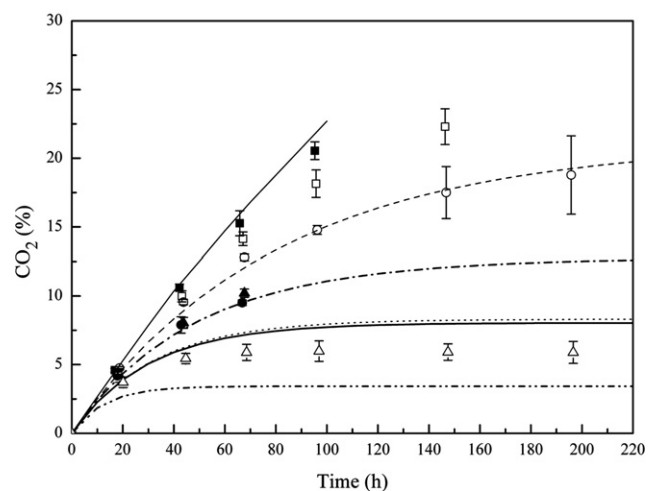


**Fig. 11.** Experimental and predicted evolution of CO<sub>2</sub> composition for different 'Andross' peach packages: without microperforation (■, continuous line), one 90 × 50 μm hole (□, dash line), two 90 × 50 μm holes (○, dash dot line), one 210 × 135 μm hole (●, dot line), two 125 × 75 μm holes (▲, continuous thick line), three 200 × 100 μm holes (Δ, dash dot dot line).

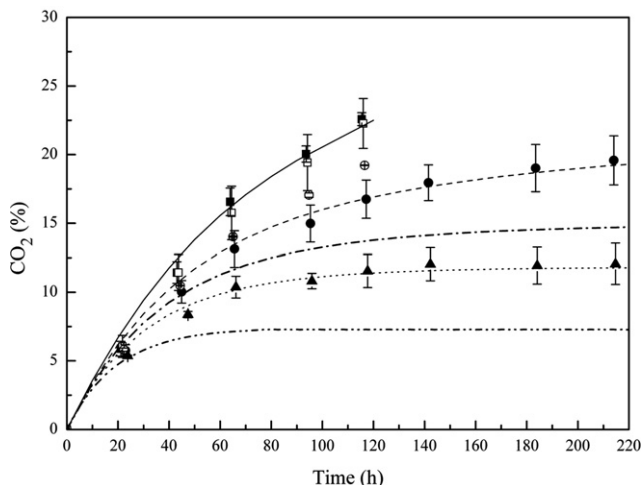


**Fig. 12.** Experimental and predicted evolution of CO<sub>2</sub> composition for different 'Calante' peach packages: without microperforation (■, continuous line), one 90 × 50 μm hole (□, dash line), two 90 × 50 μm holes (◊, dash dot line), one 200 × 130 μm hole (●, dot line), two 200 × 120 μm holes (▲, dash dot dot line).

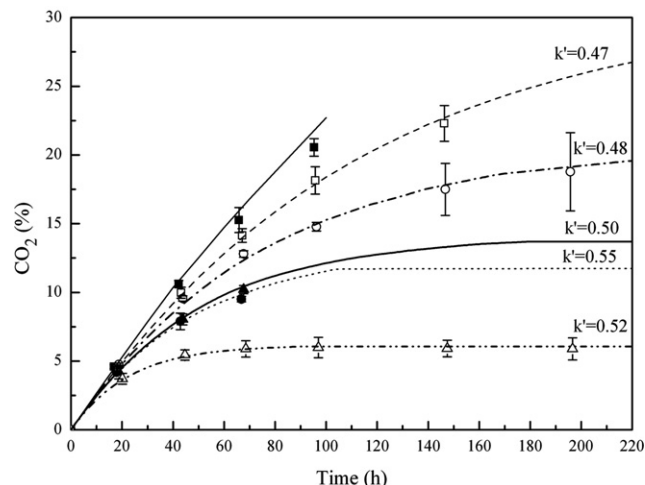


**Fig. 14.** Experimental and predicted evolution of CO<sub>2</sub> composition, modified with a correction factor, for different 'Andross' peach packages: without microperforation (■, continuous line), one 90 × 50 μm hole (□, dash line), two 90 × 50 μm holes (◊, dash dot line), one 210 × 135 μm hole (●, dot line), two 125 × 75 μm holes (▲, continuous thick line), three 200 × 100 μm holes (Δ, dash dot dot line).

opposite direction, it ought to be possible to model the CO<sub>2</sub> concentration correctly. A product such as the truffle whose CO<sub>2</sub> production exceeds its O<sub>2</sub> consumption could approach the conditions of this supposition. The respiratory coefficient of the truffle is higher than 1 and therefore the hydrodynamic flow would go from the interior to the exterior of the package. Theoretically, the O<sub>2</sub> exchange through the microperforation could be difficult in this case, but is unlikely in fact due to the continuous movement of air in the storage rooms where the product is kept. The experimental evolution of the CO<sub>2</sub> in the packages with truffle coincides with the model predictions, Fig. 13. This appears to suggest that the reasons for the lack of agreement between the experimental and calculated values are those given above.

The value of a correction factor,  $k'$ , has been estimated by which the transmission rate of the CO<sub>2</sub>,  $TR_{CO_2}$ , should be multiplied in order to obtain the correct fit of the experimental results. For the three products with respiratory coefficients lower than 1, and for all the films used, the value of  $k'$  was between 0.40 and 0.55. Figs. 14 and 15 show the evolution of the CO<sub>2</sub> pre-

dicted by the model modified with the correction factors for 'Andross' and 'Calante' peaches, respectively. Despite the fact that the consumption and transmission rates of O<sub>2</sub> do not depend on the CO<sub>2</sub> concentration, the oxygen concentration can be seen to be slightly modified by a change in the CO<sub>2</sub> composition. This is due to the fact that a greater accumulation of CO<sub>2</sub>, originated by the inclusion of the correction term  $k'$ , produces a reduction in the difference of pressure between the interior and the exterior, and therefore in a higher hydrodynamic flow. However, this influence is very small and in all cases the term  $k'$  modifies the evolution of the O<sub>2</sub> concentration by less than 3.2%. Obviously the introduction of a correction factor, although useful, should be considered as a temporary solution. Future models need to be developed that are devoid of such factors in which the dependence of the concentration of the different gases with the spatial coordinates is taken into account.

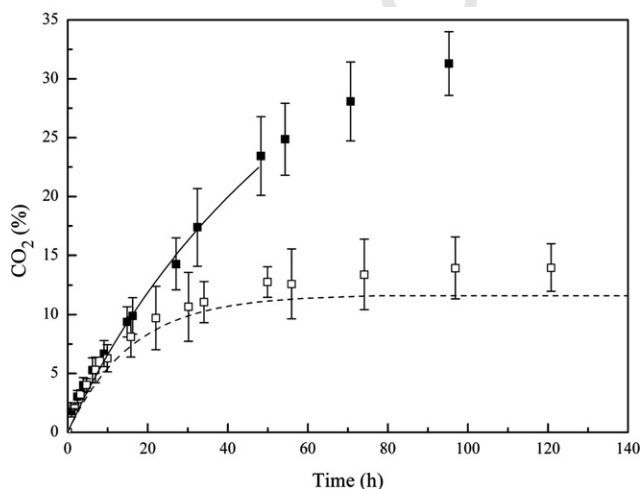


**Fig. 13.** Experimental and predicted evolution of CO<sub>2</sub> composition for black truffle packages: without microperforation (■, continuous line), two 90 × 50 μm holes (□, dash dot line).

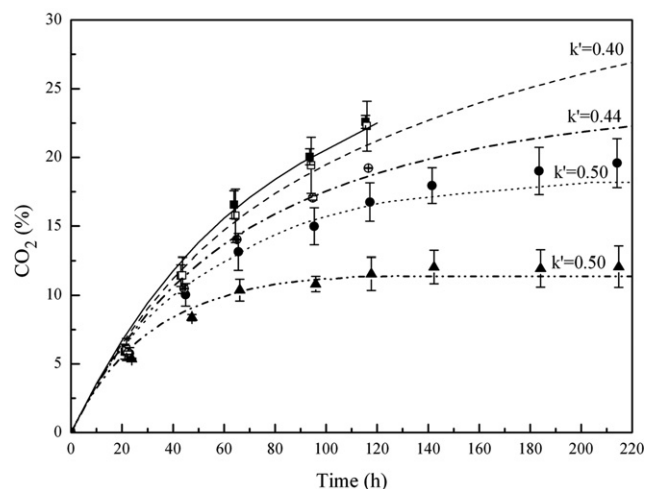


**Fig. 15.** Experimental and predicted evolution of CO<sub>2</sub> composition, modified with a correction factor, for different 'Calante' peach packages: without microperforation (■, continuous line), one 90 × 50 μm hole (□, dash line), two 90 × 50 μm holes (◊, dash dot line), one 200 × 130 μm hole (●, dot line), two 200 × 120 μm holes (▲, dash dot dot line).

#### 4. Conclusion

The model proposed for describing the evolution of the gas composition in packages with microperforated films and with constant volume, taking into account the permeation through the films, the diffusive and hydrodynamic flow through the microperforations and the respiration rate of the packaged product, is a useful tool for predicting the evolution of O<sub>2</sub> composition. The predictions of the model represent an acceptable match with the experimental O<sub>2</sub> composition for all the products and packages tested. The main novelty of this model lies in the inclusion of a potential relation between the microperforation area and the transmission rate, (Eq. (5)). However, the CO<sub>2</sub> levels estimated by the model are lower than the experimental values for products with respiratory coefficients lower than 1 ('Andross' and 'Calante' peaches, and cauliflower), but in agreement when the CO<sub>2</sub> production is greater than the O<sub>2</sub> consumption (truffle). It is postulated that the reason for this is the existence of an air current flowing from outside the package that reduces the CO<sub>2</sub> concentration around the microperforation.

#### 5. Uncited references

Q1 [Haggar et al. \(1992\)](#) and [Song et al. \(1992\)](#).

#### Acknowledgement

The authors express their gratitude to the 'Ministerio de Educación y Ciencia' (Spain) for providing the financial support for the study (Project PET 2007-009-C05-03).

#### References

- Becker, K., 1979. Water-vapor permeability of open pores and other open holes in packages. *Verpackungs Rundschau* 30 (12), 87–90.
- Bennik, M.H.J., Vorstman, W., Smid, E.J., Gorris, L.G.M., 1998. The influence of oxygen and carbon dioxide on the growth of prevalent *Enterobacteriaceae* and *Pseudomonas* species isolated from fresh and controlled-atmosphere-stored vegetables. *Food Microbiology* 15, 459–469.
- Bird, R.B., Stewart, W.E., Lightfoot, E.N., 2007. *Transport Phenomena*, revised second ed. John Wiley & Sons, New York, USA.
- Brody, A.L., 2005. What's fresh about fresh-cut. *Food Technology* 59 (1), 74–77.
- Cameron, A.C., Beaudry, R.M., Banks, N.H., Yelanich, M.V., 1994. Modified-atmosphere packaging of blueberry fruit: modelling respiration and package oxygen partial pressures as a function of temperature. *Journal of the American Society of Horticultural Science* 119, 534–539.
- Del-Valle, V., Almenar, E., Lagarón, J.M., Catalá, R., Gavara, R., 2003. Modelling permeation through porous polymeric films for modified atmosphere packaging. *Food Additives and Contaminants* 20, 170–179.
- Emond, J.P., Castaigne, F., Toupin, C.J., Desilets, D., 1991. Mathematical modeling of gas exchange in modified atmosphere packaging. *Transactions of the American Society of Agricultural Engineers* 34 (1), 239–245.
- Fishman, S., Rodov, V., Peretz, J., Ben-Yehoshua, S., 1995. Model for gas exchange dynamics in modified-atmosphere packages of fruits and vegetables. *Journal of Food Science* 60, 1078–1083.
- Fishman, S., Rodov, V., Ben-Yehoshua, S., 1996. Mathematical model for perforation effect on oxygen and water vapor dynamics in modified atmosphere packages. *Journal of Food Science* 61 (5), 956–961.

- Fonseca, S.C., Oliveira, F.A.R., Chau, K.V., 1996. Modeling oxygen and carbon dioxide exchange through a perforation, for development of perforated modified atmosphere bulk packages. Abstract and Poster Session at: IFT Annual Meeting and Food Expo, June 22–26, New Orleans, USA.
- Fonseca, S.C., Oliveira, F.A.R., Frias, J.M., Brecht, J.K., Chau, K.V., 2002. Modelling respiration rate of shredded Galega kale for development of modified atmosphere packaging. *Journal of Food Engineering* 54 (4), 299–307.
- González, J., Ferrer, A., Oria, R., Salvador, M.L., 2008. Determination of O<sub>2</sub> and CO<sub>2</sub> transmission rates through microperforated films for modified atmosphere packaging of fresh fruits and vegetables. *Journal of Food Engineering* 86, 194–201.
- Geankoplis, C.J., 1993. *Transport Processes and Unit Operations*, third ed. Prentice Hall, New Jersey, USA.
- Ghosh, V., Anantheswaran, R.C., 2001. Oxygen transmission rate through microperforated films: measurement and model comparison. *Journal of Food Process Engineering* 24, 113–133.
- Gorny, J.R., Hess-Pierce, B., Kadder, A.A., 1999. Quality changes in fresh-cut peach and nectarine slices as affected by cultivar, storage atmosphere and chemicals treatments. *Journal of Food Science* 64 (3), 429–432.
- ~~Haggar, P.E., Lee, D.S., Yam, K.L., 1992. Application of an enzyme kinetics based respiration model to closed system experiments for fresh produce. *Journal of Food Process Engineering* 15, 143–157.~~
- Heiss, R., 1954. *Verpackung Feuchtigkeitsempfindlicher Lebensmittel*. Springer, Berlin, Germany.
- Hernandez, R.J., 1997. Food packaging materials, barrier properties, and selection. In: Valentas, K.J., Rotstein, E., Singh, R.P. (Eds.), *Food Engineering Practice*. CRC Press, Boca Raton, FL, USA, pp. 291–360.
- Iqbal, T., Rodrigues, F.A.S., Mahajan, P.V., Kerry, J.P., 2009. Mathematical modeling of the influence of temperature and gas composition on the respiration rate of shredded carrots. *Journal of Food Engineering* 91, 325–332.
- Kader, A.A., 1987. Respiration of gas exchange of vegetables. In: Weichmann, J. (Ed.), *Postharvest Physiology of Vegetables*. Marcel Dekker, New York, USA, pp. 25–43.
- Kader, A.A., Zagory, D., Kerbel, E.L., 1989. Modified atmosphere packaging of fruits and vegetables. *Critical Reviews in Food Science and Nutrition* 28 (1), 1–30.
- Lange, J., Büsing, B., Hertlein, J., Hediger, S., 2000. Water vapour transport through large defects in flexible packaging: modeling, gravimetric measurement and magnetic resonance imaging. *Packaging Technology and Science* 13, 139–147.
- Mannapperuma, J.D., Zagory, D., Singh, R.P., Kader, A.A., 1989. Design of polymeric packages for modified atmosphere storage of fresh produce. In: Fellman, J.K. (Ed.), *Proceedings of the Fifth International Controlled Atmosphere Research Conference*, vol. 2. Wenatchee, Washington, USA, pp. 359–366.
- Martinez, J.A., Chiesa, A., Tovar, F., Artés, F., 2005. Respiration rate and ethylene production of fresh cut lettuce as affected by cutting grade. *Agricultural and Food Science* 14, 354–361.
- Paul, D.R., Clarke, R., 2002. Modeling of modified atmosphere packaging based on designs with a membrane and perforations. *Journal of Membrane Science* 208, 269–283.
- Philips, C., 1996. Review: modified atmosphere packaging and its effects on the microbiological quality and safety of produce. *International Journal of Food Science and Technology* 34, 463–479.
- Salvador, M.L., Jaime, P., Oria, R., 2002. Modeling of O<sub>2</sub> and CO<sub>2</sub> exchange dynamics in modified atmosphere packaging of burlat cherries. *Journal of Food Science* 76, 231–235.
- Silva, F.M., Chau, K.V., Brecht, J.K., Sargent, S.A., 1999. Tubes for modified atmosphere packaging of fresh fruits and vegetables: effective permeability measurement. *Applied Engineering in Agriculture* 15 (4), 313–318.
- ~~Song, Y., Kim, H.K., Yam, K.L., 1992. Respiration rate of blueberry in modified atmosphere at various temperatures. *Journal of the American Society for Horticultural Science* 117 (6), 925–929.~~
- Talasila, P.C., Cameron, A.C., Joles, D.W., 1994. Frequency distribution of steady-state oxygen partial pressures in modified-atmosphere packages of cut broccoli. *Journal of the American Society of Horticultural Science* 119, 556–562.
- Watada, A.E., Ko, N.P., Minott, D.A., 1996. Factors affecting quality of fresh-cut horticultural products. *Postharvest Biology and Technology* 9, 115–125.
- Yam, K.L., Lee, D.S., 1995. Design of modified atmosphere packaging for fresh produce. In: Rooney, M.L. (Ed.), *Active Food Packaging*. Chapman & Hall, Glasgow, United Kingdom, pp. 55–73.